

GT2011-46856

## Forced Response Prediction for Steam Turbine Last Stage Blade Subject to Low Engine Order Excitation

**Bin Zhou**  
**Amir Mujezinovic**  
**Andrew Coleman**  
GE Energy  
Schenectady, NY, USA

**Wei Ning**  
GE Energy  
Greenville, SC, USA

**Asif Ansari**  
GE Energy  
Bangalore, Karnataka, India

### ABSTRACT

Low Engine Order (LEO) excitations on a steam turbine Last Stage low-pressure (LP) Bucket (or Blade) (LSB) are largely the result of flow unsteadiness (e.g. flow circulation and reversal) due to low steam exit velocity ( $V_{ax}$ ) off the LSB at the off-design conditions. These excitations at low frequencies impose major constraints on LP bucket aeromechanical design. In this study, bucket forced response under typical LEO excitation was analytically predicted and correlated to experimental measurements. First, transient CFD analyses were performed at typical low flow, low  $V_{ax}$  operating conditions that had been previously tested in a subscale low pressure turbine test rig. The unsteady pressure distribution on the bucket was derived from the transient CFD analyses at frequencies corresponding to the bucket's modes of vibration. Subsequently, these computed unsteady pressure were mapped onto a LSB finite element model, and forced response analyses were performed to estimate the bucket dynamic response, i.e. the alternating stresses and strains. The analytically predicted bucket response was compared against measured data from airfoil mounted strain gages and good correlation was found between the analytical prediction and the test data. Despite uncertainty associated with various parameters such as damping and unsteady steam forcing etc., the developed methodology provides a viable approach for predicting bucket forced response and in turn High Cycle Fatigue (HCF) capability during early phases of steam turbine LSB design.

### 1. INTRODUCTION

At off-design, low  $V_{ax}$  operating conditions, such as Full Speed No Load (FSNL) or high exhaust pressure operation, long steam turbine LSBs experience unique steam flow conditions characterized by substantial hub separation, flow circulation and reversal, as well as transonic to supersonic tip flow velocity. These flow conditions result in broad band

stimuli that lead to forced vibrations of the bucket in low frequency regime, i.e. in bucket's fundamental modes. As a result, bucket HCF failure may occur under a combination of mean stresses and significant alternating stresses. Analytical prediction of bucket alternating stresses under various flow conditions is, in general, still a significant challenge, since sufficient accuracy and repeatability are not always ensured. Therefore, rigorous analytical determination of the alternating stress, in particular at off-design operating conditions, is not yet factored directly into a standard industry-wide turbine blading design practice. In most cases, steam turbine buckets are designed to avoid major resonant responses at turbine running speed. Alternating stresses and HCF capability of a new design can only be measured in an engine test through strain gauged components, after the design work has been largely completed. The ability to predict forced response of buckets under unsteady aerodynamic loading and subsequently perform HCF assessment during a design phase brings great benefits to turbomachinery manufacturers. It would result in a broader design space where, in some cases, bucket behavior at off-design operating conditions can be analytically examined, and in other cases certain resonant responses can be potentially tolerated based on the predicted response level. Advanced aeromechanics analysis methodologies such as forced response prediction would in turn enable a higher efficiency bucket design.

Blade forced response under aerodynamic forcing, especially LEO excitations, has been studied by a number of research groups in past decades. Breard et al.<sup>1</sup> showed comparable response amplitude due to either LEO excitation or excitations at blade/nozzle passing frequencies (BPF/NPF), and indicated that nearly half of all HCF issues are caused by LEO excitation based on actual engine experiences. One major source of LEO excitations has been identified as loss of flow symmetry caused by a number of reasons including inlet

distortions, blade count difference through multiple stages, throat variations of stator vane (nozzle), circumferential non-uniformity of flow injections such as cooling flows and of the non-uniform temperatures at combustor exit (Breard et al.<sup>1</sup>, Marshall et al.<sup>2</sup>, Vahdati et al.<sup>3</sup>, Manwaring and Kirkeng<sup>4</sup>), Stimuli induced by any protrusions or openings in the flow path such as steam extractions, drainage, struts, joints, probes etc. also belong to this broad category. Nevertheless, LEO excitation as a result of significantly low  $V_{ax}$  and/or high exhaust pressure at LSBs of a steam turbine is least studied due to complexity of flow physics.

There are two major types of forced response methodologies, namely fully coupled fluid-structure analysis and loosely or sequentially coupled analysis. Breard et al.<sup>1</sup>, Marshall et al.<sup>2</sup>, Vahdati et al.<sup>3</sup> for example, used the first approach where structural mode shapes are interpolated onto aerodynamic mesh which moves at each time step according to the structural motion. Thus, unsteady forcing and structure vibration are allowed to interact in these time-marching computational schemes. These models however are often fully 3D with whole annulus geometries and sometime multistage as well, therefore are prohibitively expensive to run. Moffatt et al.<sup>5</sup> and Ning et al.<sup>6</sup> on the other hand, applied a more computationally efficient method in a frequency domain for aeroelastic calculations, where aerodynamic forcing is calculated without input of blade vibration and is only subsequently coupled with structural model to predict blade response. This approach, often combined with so called single degree of freedom (SDoF) linear response prediction formulation, was also adopted by Manwaring and Kirkeng<sup>4</sup> to calculate the stress on a LPT blade due to temperature distortion induced LEO excitation. Using measured temperature, pressure, and damping, they were able to predict alternating strains that reasonably match the measured values. Particularly suitable for blades with lower vibratory amplitude, this method was also reported widely in other works such as Kielb<sup>7</sup>, Chiang and Kielb<sup>8</sup>, and was in many cases proved to be computationally efficient. A significant extension of sequentially coupled forced response methodology includes advanced formulations of nonlinear frictional damping that computes frictional damping along with damped forced response with given aerodynamic excitations (Yang and Meng<sup>9</sup>, Peng and Petrov<sup>10</sup>, Poudou and Pierre<sup>11</sup>). Forced response prediction with such analytically computed frictional damping and aerodynamic damping (via calculation of energy transfer between fluid and structure in CFD analysis) provides enhanced analytical response prediction capability.

In this work, sequentially coupled forced response approach with a linear SDof model was adopted. Total damping was extracted from existing turbine test data. The LEO excitations under low  $V_{ax}$  steam turbine operating conditions in the last stage bucket was captured using unsteady CFD. Then the bucket forced response with resolved LEO excitation was calculated with a harmonic response analysis in a frequency

domain. The predicted bucket responses in terms of airfoil strains were compared to measured engine test data.

## 2. RESPONSE PREDICTION METHODOLOGIES

The process flow of the employed forced response scheme is shown below in Figure 1.

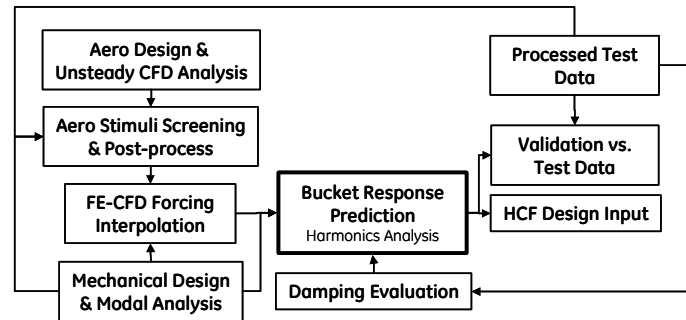


**Figure 1: Flow Chart of Forced Response Methodology**

The process can normally start with structural modal analysis and transient CFD analysis in parallel. A Campbell diagram is created from blade structural analysis as resonant frequencies at different nodal diameters (responding to respective engine orders) are predicted. On the other hand, at the convergence of the transient CFD analysis, unsteady pressure history on the airfoil surfaces can be transformed into a frequency domain. Frequency-spectrums of local pressure history or integrated airfoil surface force or moment are examined to identify significant stimuli that could couple with predicted bucket modal frequencies and drive the response of respective vibratory modes. Depending on data availability, such a screening process can also be held against bucket response frequencies measured in a turbine test. Upon completion of the screening, 3D pressure distributions at frequencies or engine orders of interest can then be extracted.

A subsequent and critical step is to interpolate unsteady pressure and vibration mode shape between CFD and structural models. This interpolation is used to derive a forcing function or so called modal force in the modal domain. Such interpolations can be done in either direction, i.e. mapping of unsteady pressure on finite element grid or mapping mode shapes on the CFD mesh. Generally, cautions and engineering judgments are required in the interpolations due to discrepancies between CFD and structure models, such as mesh types and mesh densities. The accuracy of interpolation is critical for accurate model force calculations.

After modal force is obtained, response prediction for the bucket can be done following the SDof approach in several formats, all of which are essentially harmonic analysis where forcing and response are represented as harmonics in a frequency domain. Damping is required in a harmonic analysis and it can be obtained from either test data or analytical tools.

This forced response prediction method has also been demonstrated in validations against test measurements by several groups (Manwaring and Kirkeng<sup>4</sup>, Moffatt et al.<sup>5</sup> and Ning et al.<sup>6</sup>, Kield<sup>7</sup>, Chiang and Kield<sup>8</sup>). In our work, this method has been applied for the analysis of a particular steam turbine last stage bucket and is presented in the following sections.

## 2.1 Turbine Test and Response Data

Authors' company steam turbine engineering has been validating bucket aeromechanical designs in a Low-Pressure Development Turbine (LPDT) testing facility for a number of years. This facility (Figure 2) is capable of running a wide range of inlet and exhaust steam conditions for the testing of subscale LP section steam turbines. The main test objectives include testing the LP buckets in extended turbine operating envelop and providing validation for advanced analytical aeromechanics design and analysis tools. For the latter purpose, correlation between measured responses frequency and amplitude with analytical calculations are often sought.



**Figure 2: GE LPDT Testing Facility**

The particular bucket of interest in this work is a steam turbine LSB of modern design as shown in Figure 3. This bucket features an integral tip shroud, a mid-span nub/sleeve connection and a curved axial dovetail. Both tip and part span connections provide frictional damping and structural support. A turbine LP section with several stages of subscale buckets including the LSBs were instrumented with strain gages at desired locations on selected buckets and tested over various flow conditions in the test facility. The LSBs were instrumented with strain gages mounted on five airfoil locations. The number of instrumented buckets around the wheel for a given gage location, i.e. the circumferential redundancy of a particular gage location, is between 4 and 10. Figure 3 also shows an experimental Campbell diagram derived from the test. Extensive EO2 (2/rev) response corresponding to the 1<sup>st</sup> axial mode of the bucket can be clearly observed.

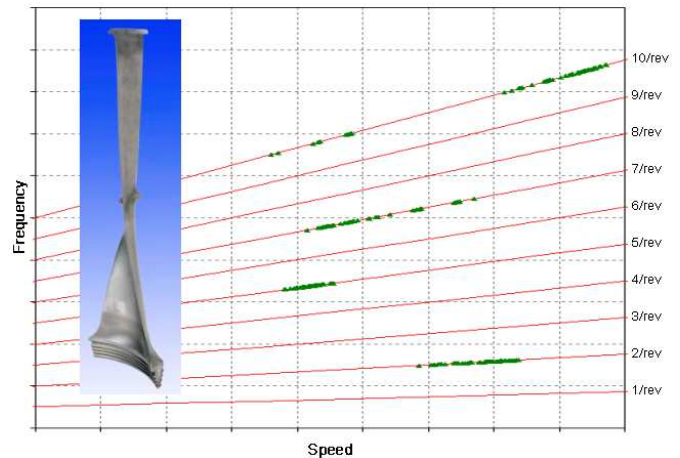


**Figure 3: GE LSB and LPDT Test Campbell Diagram**

A matrix of Test Points (TPs) spans wide envelope, each representing a typical flow condition defined by mass flow and exhaust pressure. At each test point, i.e. a particular operating condition, turbine speed was controlled to sweep through a wide speed range and to dwell at a designed running speed. In this study, two test points were selected to validate the forced response analytical prediction, namely TP-A2 and TP-C6. These two test points represent typical low  $V_{ax}$  conditions where steam flow downstream of turbine last stage would start re-circulating below LSB tip and lead to unsteady aerodynamic stimuli to the bucket. The two test points have a similar steam exit velocity  $V_{ax}$  around 200ft/s (61m/s), with TP-C6 featuring a higher exhaust pressure roughly 3 times that of TP-A2. Figure 4 shows frequency processed EO2 bucket response during a speed sweep at a particular gage location during test point A2. Using the industry recognized half-power method, Eq. 1, the total damping was derived using the speed sweep data, similar to what is shown in Figure 4, for all working gages.

$$Q = \frac{\omega_n}{\omega_2 - \omega_1} \quad (1)$$

Damping values derived for all gages at the same airfoil location were then averaged for a particular test point. It was found that damping of test point C6 is approximately twice of that in test point A2, for all gage locations used for the calculation. It can be hypothesized that higher exhaust pressure in TP-C6 leads to an increase in the aerodynamic damping as well as a tendency to induce a higher level of bucket vibratory motion that in turn causes more frictional damping at tip and mid-span contact surfaces. Further, damping values calculated at all gage locations for a given TP distribute in a very narrow range, i.e. a  $\Delta Q$  of only 2~3. Fourier transformations were also performed on a series of time domain data at constant turbine speed for both test points. In Figure 5, maximum peaks of frequency response can be seen for both test points corresponding to the bucket 1<sup>st</sup> axial mode, consistent with what is shown in the test Campbell diagram. Response spectrums are fairly similar between two TPs, both show a broad band

vibrations with dominant 1<sup>st</sup> axial mode response representing up to ~40% of the total gage response observed in the time domain.

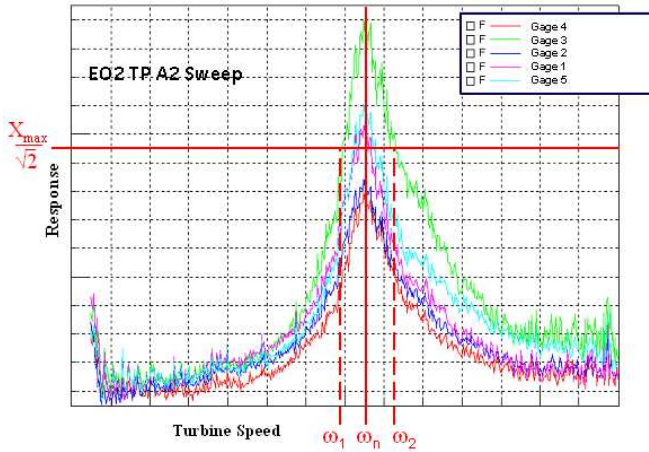


Figure 4: EO2 Gage Response during Speed Sweep

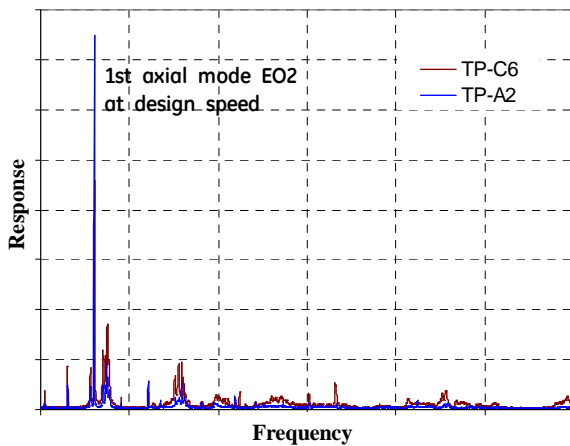


Figure 5: Responses Shown in a Frequency Spectrum

## 2.2 Transient CFD Analysis and Stimuli Screening

Viscous transient CFD analysis was performed on a sector model built with a proprietary code. The code is a 3D structured grid, non-linear and linear Euler/Navier-Stokes solver for turbomachinery rows. The sector model has 23M nodes, consisting of multiple passages of the last stage nozzles and buckets (Figure 6). A simplified LSB tip shroud was modeled to account for tip flow blockage. The exhaust domain was extended to simulate the down flow exhaust hood. Boundary conditions at inlet and exhaust were set to match the LPDT test conditions. A separate single passage, multi-stage steady state model was used to determine the initial conditions of the transient analysis. As shown in Figure 7, the steady state flow structure at test point A2 indicates that ~80% of the steam passes through above ~70% span of the bucket, whereas rest of the flow circulates and reverses at the backside of the LSB. To

capture flow physics and produce fine enough frequency resolution, multiple turbine revolutions were completed in the transient aerodynamic analysis. History of integrated unsteady pressure for test point A2 is shown in Figure 9, constructed by integrating the surface pressure, shown in Figure 8, for all time steps. The last two or so revolutions showed apparent periodicity and indicated the convergence of the transient solution, therefore were used in Fourier transformation and converted into frequency domain. Figure 10 shows frequency spectrums of unsteady pressures at a series of locations along the entire length of the bucket airfoil. Besides clear peaks corresponding to harmonics of NPF, tip shedding due to vortex formation upstream of LSB tip shroud is also shown. Most importantly, a zone of LEO or low frequency excitations can be clearly observed in the spectrum, among which a stimulus at essentially EO2 frequency is present (most probably causing the 1<sup>st</sup> Axial mode EO2 response shown in Figure 5). Only the lower half of the bucket is exposed to LEO excitations, where flow separation and circulation exist. Tip shedding frequency and NPFs are mostly dominant at regions near bucket tip. In conjunction with experimental Campbell diagram (Figure 3) and strain gage response data (Figure 5), 3D airfoil unsteady distributions at this excitation frequency were extracted and served as inputs to harmonic forced response analysis. Figure 8 shows the amplitude of unsteady pressure distribution on the pressure side of the bucket at TP-A2. In correlation with a steady flow plot in Figure 7, a distinctive vortex can be seen and the flow migrates radially up on the pressure side of the bucket. This vortex together with the flow separation at the LSB lower hub region were believed to have led to the EO2 excitation. Similar flow characteristics were also found for TP-C6, with an overall significantly higher level of unsteady pressure amplitude.

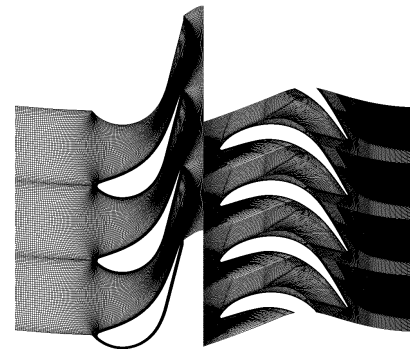


Figure 6: Transient CFD Computation Domain (top view)

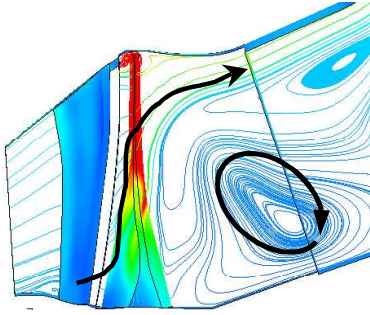


Figure 7: Steady Flow Structure of TP-A2

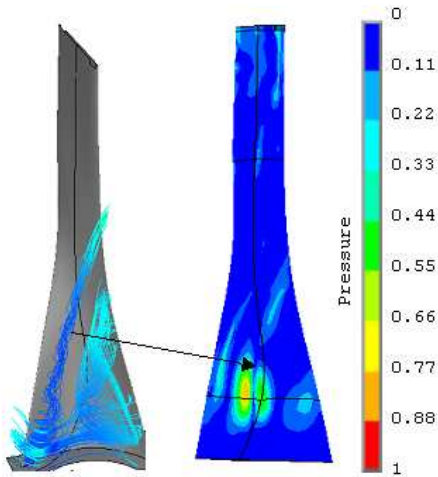


Figure 8: EO2 Unsteady Pressure Distribution at Pressure Side, TP-A2

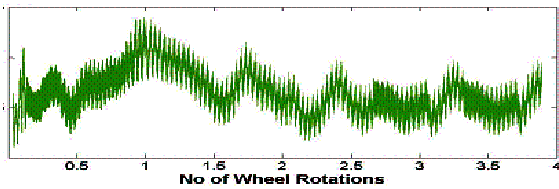


Figure 9: Integrated Bucket Surface Unsteady Pressure, TP-A2

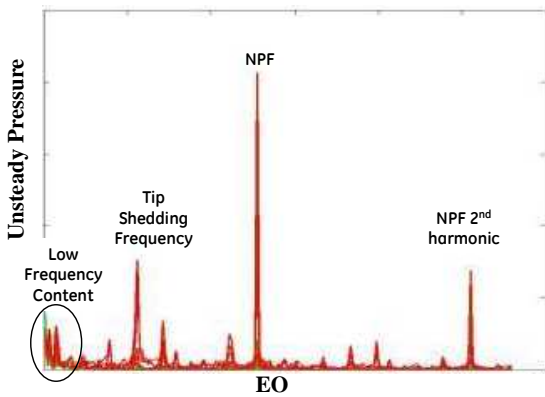


Figure 10: Frequency Spectrum of Unsteady Pressures, TP-A2

### 2.3 FE Modeling and Forced Response Prediction

A cyclically symmetric finite element model was built for the studied LSB (Figure 11). The model was first used to predict bucket modal frequencies. The 1<sup>st</sup> axial mode at 2-nodal diameter pattern (ND2) in the model closely matches the experimental response frequency (Figure 11). It is believed that the coupling between this mode and the EO2 excitation at essentially the same frequency excited the axial mode in the LPDT test.

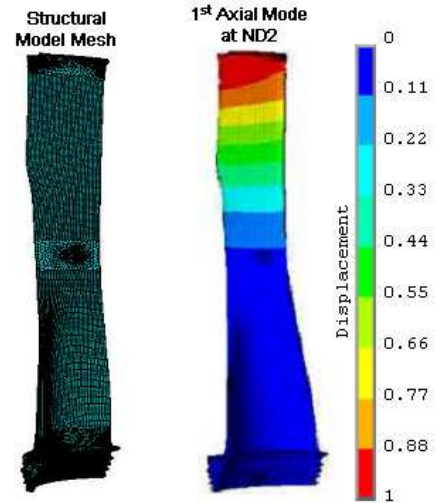


Figure 11: Structural Model and 1<sup>st</sup> Axial Mode Shape

Generic finite element harmonic analysis module available in ANSYS<sup>®</sup>-12 was used in the forced response prediction. ANSYS<sup>®</sup>-12 is the first version of ANSYS that provides the capability of calculating multiple nodal diameter structure response using a cyclic symmetry model. This feature was explored and validated with extensive studies. It was then used in this work to avoid costly full wheel calculation of the structure. Solving forced response directly in ANSYS requires unsteady pressure distributions from CFD analysis to be interpolated or mapped onto finite element mesh, as previously discussed. It should be noted that due to the complex nature of pressure distributions, both real and imaginary pressure components are to be applied on the bucket surfaces of the finite element model. Further, phase shifts of the unsteady pressure around the wheel were applied in the pressure mapping process. As shown in Eq. 2,  $P_j$  represents pressure at  $j^{\text{th}}$  bucket,  $\phi$  is the phase shift from bucket #1 and IBPA is the commonly known intra-blade phase angle.

$$P_j = P_1 \cdot e^{i\phi}, \phi = \text{IBPA} \cdot (j - 1) \quad (2)$$

A harmonic analysis was performed across a narrow frequency range in the vicinity of the resonance determined from earlier finite element modal analysis. Total damping was calculated from the actual gage responses recorded in LPDT test (as discussed above). Figure 12 shows the contour of predicted

alternating stresses on the bucket normalized to the maximum value, on both pressure and suction sides.

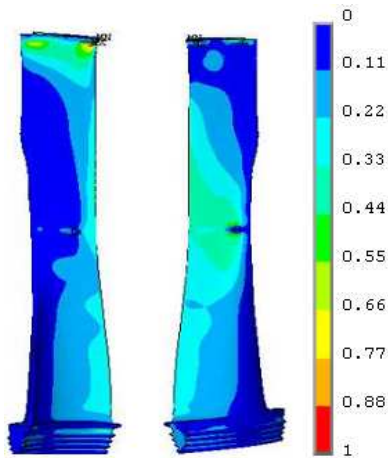


Figure 12: Bucket Alternating Stresses

### 3. COMPARISON: PREDICTION AND MEASUREMENT

Strain components at five strain gage locations were extracted from the results of harmonic analysis and compared with measured data. While the response prediction was essentially deterministic in nature, uncertainty factors could have been applied on the prediction. These factors normally include mistuning induced bucket-to-bucket response variation and instrumentation error etc., but were not applied in the present study. Forced response predictions for EO2, 1<sup>st</sup> axial mode are shown in Figure 13 and Figure 14, along with actual strain gage readings (ranges and mean values) at five strain gage locations all normalized to the maximum recorded response. The spread in gage readings among the gage positions is simply due to the gages being in different physical locations around the LSB; with the mode shape determining the relative response amplitude. The ranges of readings also vary from location to location due to the local strain gradient of the responding mode. If a gage is placed in high strain gradient location, small variances in the bucket-to-bucket gage locations will show up as a larger range of responses. Larger ranges can also be attributed to the effects of mistuning, as each LSB will not have the same peak response. The effects of mistuning were not studied in this work and represent a potential for future investigation.

Overall, a very good correlation can be found between the predicted response and measured data. Responses at most gage locations were underestimated for test point A2, and overestimated for test point C6. Significant differences in predicted unsteady pressure amplitude between the two test points are believed to be the major factor driving the differences in predicted responses. At the same time, engine test data show less difference between the responses at the two test conditions.

Some potential reasons for the discrepancy between measured and predicted responses are discussed below.

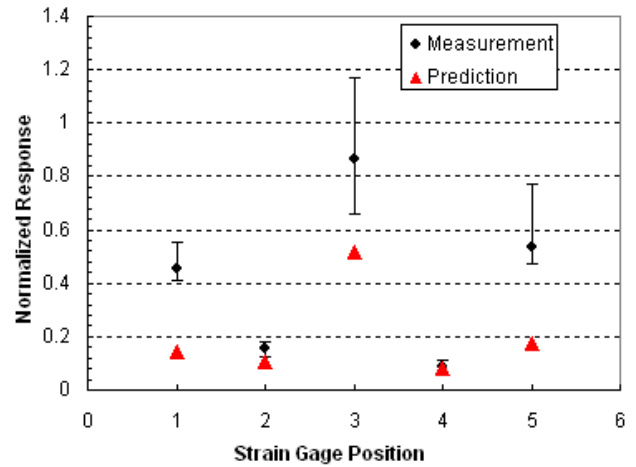


Figure 13: Response Prediction TP-A2

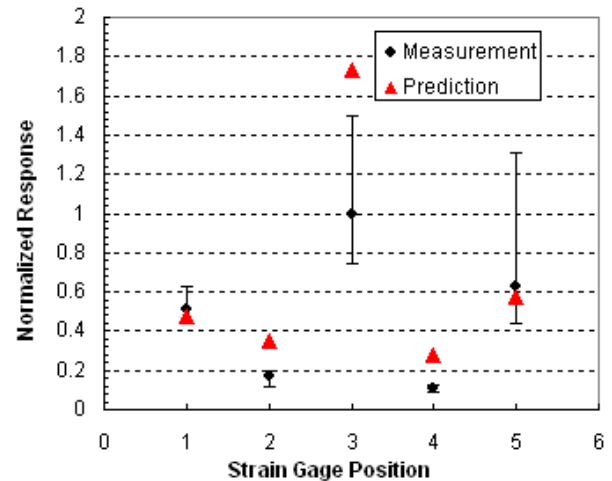


Figure 14: Response Prediction TP-C6

### 4. CONCLUSIONS

A practical forced response scheme using a generic ANSYS harmonic analysis in combination with the forcing functions provided by unsteady CFD analysis is presented. The methodology consisting of a set of different analyses and screening processes was able to capture the LEO excitation to the steam turbine LSB as a result of flow unsteadiness downstream of the LSB at typical low  $V_{ax}$  operating conditions. Forced response predictions based on calculated LEO excitation were well correlated with measured strain gage data. Uncertainties listed below can contribute to the discrepancies between the predictions and measurement:

- Inaccuracy of the transient CFD to capture large scale unsteady flow separations;
- Inaccuracy of the finite element based structural analysis results in terms of bucket mode shapes and responses, due

to potential issues in modeling such as mesh and boundary condition setup;

- Errors introduced during interpolations between CFD and FE grids;
- Uncertainties in gage location determinations either on test bucket or on a numerical bucket model, especially for high strain gradient locations;

Improvements for the methodology should be planned in the future to address the list of issues discussed above. Nonetheless, this study shows that presented methodology provides a viable approach for bucket forced response prediction. Further, with available material HCF limits and easily calculated mean stresses, assessment of bucket HCF capability can be done during early phases of the design cycle.

## ACKNOWLEDGMENTS

The authors sincerely thank Clint Ingram, Soumyik Bhaumik, Lakshmanan Valliappan, Paul Dausacker, Xiaoyue Liu, Kevin Barb, Jarfar P, and Moorthi Subramaniyan (all of General Electric Company) for their generous supports during the study.

## REFERENCES

1. Breard, C.; Green, J.S.; Imregun, M.; 2003, "Low Engine Order Excitation Mechanisms in Axial Flow Turbomachinery", *Journal of Propulsion and Power*, Vol.19, No.4, July-August, 2003
2. Marshall, J.G.; Chew, J.W.; Xu, L.; Denton, J.; 2000, "Prediction of Low Engine Order Inlet Distortion Driven Resonance in a Low Aspect Ratio Fan"; ASME paper 2000-GT-0374
3. Vahdati, M.; Sayma, A.; Imregun, M.; 1998, "Prediction of High and Low Engine Order Forced Responses for an LP Turbine Blade"; AIAA paper no AIAA-98-3719, 1998
4. Manwaring, S.R.; Kirkeng, K.L.; 1997, "Forced Response Vibrations of a LP Turbine Due to Circumferential Temperature Distortions"; *Proceedings of the 8th International Symposium on Unsteady Aerodynamics, Aeroacoustics and Aeroelasticity of Turbomachines*, Stockholm, Sweden, Kluwer Academic Publishers, ISBN0-7923-5040-5
5. Moffatt, S.; He, L.; 2003, "Blade Forced Response Prediction For Industrial Gas Turbines Part I: Methodologies", *Proceedings of ASME Turbo Expo 2003, International Gas Turbine & Aeroengine Congress & Exhibition*, June 16-19, 2003, Atlanta, Georgia, USA
6. Ning, W.; Moffatt, S.; Li, Y.S.; Wells, R.G.; 2003, "Blade Forced Response Prediction For Industrial Gas Turbines Part I: Methodologies", *Proceedings of ASME Turbo Expo 2003, Power of Land, Sea and Air*, June 16-19, 2003, Atlanta, Georgia, USA
7. Kielb, R.E., 1999, "Forced Response Design Analysis", VKI Lecture Series, 1999-05
8. Chiang, H.-W.D.; Kielb, R.E., 1992, "An Analysis System for Blade Forced Response", ASME 92-GT-172
9. Yang, B.D.; Meng, C. H.; 2005, "Characterization of Contact Kinematics and Application to the Design of Wedge Dampers for Turbomachinery Blading: Part 2-Prediction of Forced Response and Experimental Verification", *Transactions of the ASME*, Vol. 120, April 1998
10. Peng, C.; Petrov, E.; 2005, "Prediction of Mechanical Damping for Core Compressor Blades and Vaxes", 10th National Turbine Engine High Cycle Fatigue (HCF) Conference, March 8-11, 2005, New Orleans, USA
11. Poudou, O.; Pierre, C.; 2003, "Hybrid Frequency-time Domain Methods for the Analysis of Complex Structural Systems with Dry Friction Damping", *Proceedings of the 44-th AIAA/ASME/ASCE/AHS Structures, Structural Dynamics and Materials Conference*, paper AIAA2003-1411